CrossMark

ORIGINAL ARTICLE

Hydrogeochemical characterization and groundwater quality assessment in the intensive agricultural zone of the Upper Cheliff plain, Algeria

Abdelkader Bouderbala[1] · Ben Youcef Gharbi[1]

Abstract The alluvial aquifer of Upper Cheliff (northern Algeria) is known for its intensive agricultural activities, which is based especially on groundwater exploitation. This aquifer is now facing a dual problem of quantity and quality, with a decrease in the groundwater levels and an increase in mineralization. Twenty monitoring samples were collected and analyzed for major ion during the dry season 2014. In the present study, we try to characterize the hydrogeochemical processes and to assess the impact of natural and anthropogenic conditions on groundwater mineralization. The analytical results of the dry season 2014 show a groundwater quality slightly alkaline ($pH > 7$) and indicate that the majority of samples have a values exceeding the limits of potability fixed by WHO in 2008, due to the various sources of anthropogenic pollution. The Piper diagram shows the dominance of groundwater types: Ca–Cl, the mixed facies (Cl–SO$_4$–Ca–Mg), and Ca–HCO$_3$: The mineralization process in this aquifer is mainly controlled by the lithology of the aquifer (exchange water–rock and weathering of calcareous crust dissolution in the unsaturated zone), by anthropogenic factors (discharges of untreated urban sewage, intensive use of fertilizers in agriculture and the use of domestic septic tanks by rural inhabitants) and also by geoclimatic conditions (semiarid climate). Suitability of groundwater shows more than 80% of samples have very poor quality for drinking and more than 20% of samples indicate a quality unsuitable for irrigation.

Introduction

Algeria is one of the countries which has faced water problems in these last two decades. Groundwater is considered as the main resource for supplying domestic demand and for irrigation in several cities and areas in Algeria. The low rainfall and the high evaporation make this resource often fragile and vulnerable to many sources of pollution from point or non-point sources, or a combination of both. That is why it is imperative to protect it adequately in order to minimize the risks of pollution that threaten it (Subramani et al. 2010; Pulido-Madrigal et al. 2012; Saleem et al. 2015). The hydrogeochemical study is very important, because it helps to better understand the processes which influence the groundwater chemistry, and consequently, we determine its suitability for different uses. Groundwater is usually influenced by natural and anthropogenic processes from diverse sources such as local climate variation, geological factors, the residence time of water and agricultural practices (Mondal et al. 2010; Mohsen 2011; Bouderbala 2015; Touhari et al. 2015; Raj and Shaji 2016).

Groundwater resources in northern Algeria are exploited up to more than 80%, thus putting the majority of the aquifers on overexploitation situations. It is noted that rainfall in northern Algeria has decreased during the last three decades by nearly 20% compared to the five decades preceding. However, this water resource is facing problems, including quality hazard, essentially the exposure to pollution from the intensive use of fertilizers in agriculture and the uncontrolled urban discharges. It makes the groundwater unfit for human consumption.

✉ Abdelkader Bouderbala
  a.bouderbala@univ-dbkm.dz

[1] Earth Sciences Department, University of Khemis Miliana, Khemis Miliana, Algeria

🖄 Springer

In the alluvial plain of Upper Cheliff, the source of about 70% of drinking and irrigation water supplies comes from groundwater resources. The major objective of this study is to investigate and to determine the most significant hydrogeochemical processes responsible for controlling the chemistry of groundwater and to assess the suitability of groundwater for drinking and irrigation purposes.

Study area

The Upper Cheliff plain is located approximately 120 km southwest of the capital Algiers, between latitudes 36°10′ and 36°20′ north, and longitudes 02°00′ and 02°25′ east. It covers an area of about 375 km², and it is confined between the Zaccar massif in the north and the Ouarsenis chain in the south (Fig. 1).

The Upper Cheliff plain is an agricultural vocation, with important agricultural activities, and a large number of the inhabitants live in this agricultural plain, without sewage network system, and they use the septic tanks as a way to evacuate the wastewater. Agricultural practices and untreated sewage are considered as the main sources of pollution in this aquifer, as a result of the increase in nitrogen compounds, chlorides and sulfates (Khatri and Tyagi 2015).

The study area is characterized by a Mediterranean semiarid climate, with hot dry summer and cold rainy winter. The average annual temperature and rainfall are 19 °C and 390 mm, respectively (1980–2014).

The hydrographic network in the study area is extremely dense, and the most important watercourse is wadi Cheliff. In the study area there are three dams: Ghrib, Harreza and Deurdeur; these contribute to the irrigation in of the major part of the plain with more than 20.000 ha irrigated lands. However, the groundwater of this aquifer is used mainly for drinking, irrigation and industrial purposes.

Geological context

The Upper Cheliff plain forms a syncline of west–east orientation in the Tellian atlas. The stratigraphical succession in the study area from the older to recent
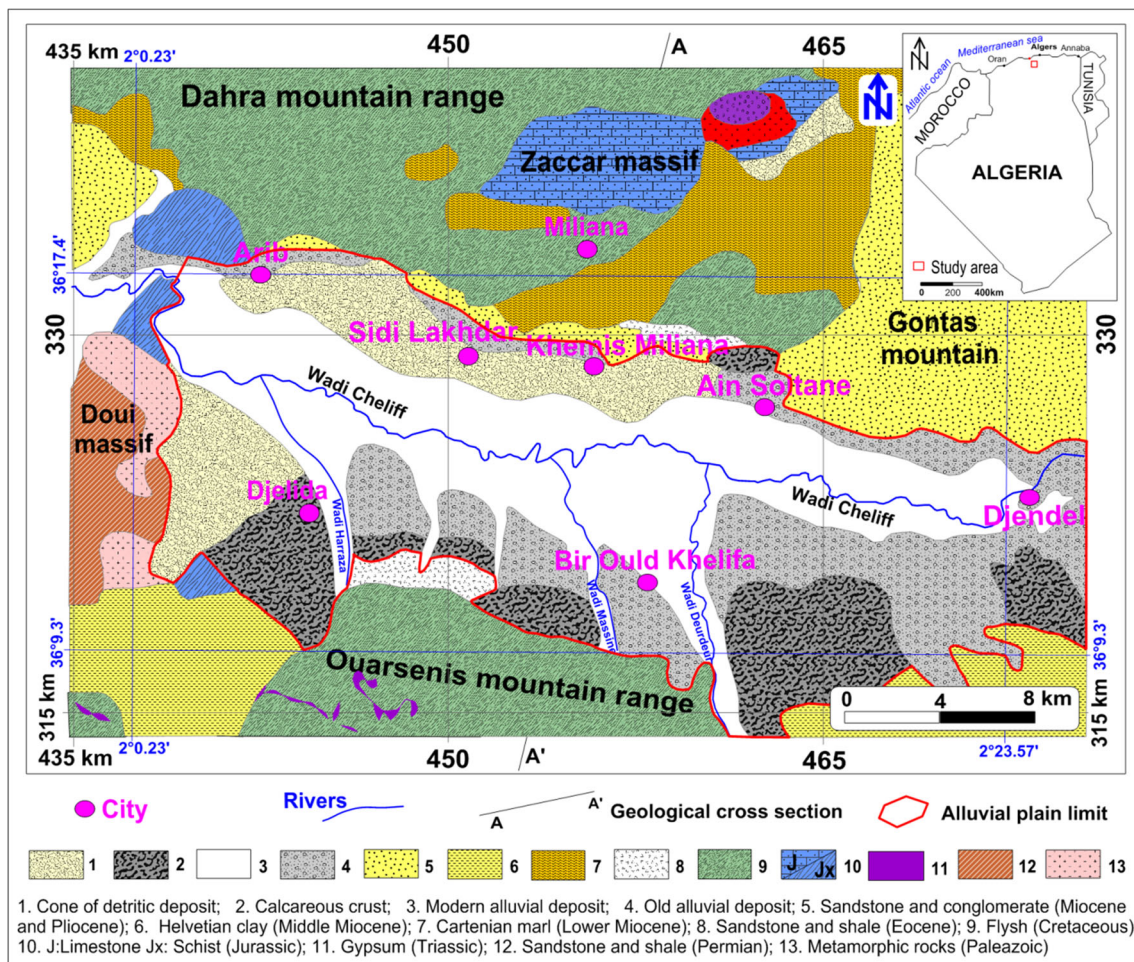

Fig. 1 Geological map of the Upper Cheliff plain. Perrodon (1957), modified

formations is the following (Perrodon 1957; Mattauer 1958; Meghraoui 1982) (Fig. 1).

The primary is observed in Zaccar and Doui massif, and it is formed by alternation of black schist, clay and quartzite. It is surmounted by the Triassic which is characterized by massive gypsum and dolomite formations, observed in Ouarsenis Mountain. The Jurassic in Zaccar massif is represented by limestone, dolomite and other carbonate rocks. However, the Jurassic formations in Doui massif are formed mainly by dolomitic limestone. The thickness of Jurassic can reach 1000 m. The Cretaceous outcrops are observed on the lateral borders of the plain, and they are mainly represented by a high series of Neocomian schist with a thickness of about 1000 m and a gray schist alternating with benches quartzite of Albian–Aptian, with a thickness near to 1000 m, and it is followed by yellowish limestone of the Senonian. The Miocene formation of 300 m of thickness begins with the Lower Miocene which is essentially formed by blue marl and clay, followed by the Middle Miocene that is represented mainly by clay, marl and some passages of sandstone and conglomerate. The Mio-Pliocene is formed mainly by limestone, sandstone, conglomerate and clay; it is observed mostly in Gontas Mountain, with a thickness about 100 m.

The Quaternary formations are mainly represented by the old alluvial deposits which are formed by conglomerate and pebble. The Calcareous crust is formed by calcareous tufa whitish, compact or powdery; it is especially developed in the southern boundary of the Cheliff plain. The alluvial fans are developed on the slopes in the boundary of the plain. The recent alluvial deposits are formed by pebble, gravel, clay and silt covered by an organic soil. There is also the alluvial plain observed just near to wadi Cheliff beds.

Hydrogeological setting

The main aquifer in the Upper Cheliff plain is formed by alluvial deposits, including pebble, gravel, sand and clay formations, with a thickness can reach 150 m. It is a locally confined aquifer, because it is covered by silt and clay on the surface, from 5 to 20 m of thickness in the center of the plain. The alluvial aquifer is overlain by the Mio-Pliocene formations, where the sandstone is apparent in the northeast at Gontas Mountain, and in the southeast of the city Djendel. In both zones, several wells are drilled and they have a good groundwater quality, and they can reach 200 m of thickness (Bouderbala 2017).

The system aquifer in this plain can be considered as multilayered aquifer systems. The hydraulic continuity between the alluvial aquifer and Mio-Pliocene aquifer exists only in the borders of the plain where there is a contact between the two aquifers without impermeable layer between them; however, in the center of the plain there is a thick clay layer between the two aquifers. We note here that we are only interested in the quaternary alluvial aquifer (Fig. 2).

The groundwater of this alluvial aquifer flows toward the center of the plain where the main drainage axis is located, which coincides with wadi Cheliff, with a main flow is from east to west. The depth of water table varies from 5 m in the west zone (near to Djelida and Arib cities) to 30 m in the east zone (near to Djendel city), while in the central part of the plain the depth of the water table levels is about 10 m (Fig. 3).

Methodology

A total of 20 groundwater samples were collected from wells in the study area during September 2014 (dry period). Bottles that are used for collecting groundwater samples were cleaned by rinsing them with distilled water. The temperature, pH, electrical conductivity (EC) and total dissolved solids (TDS) were measured in the field by using WTW Multi-parameter portable meter Multi 3430. The samples were then analyzed in the laboratory of National Agency of Hydraulic Resources (ANRH-Blida) and in the
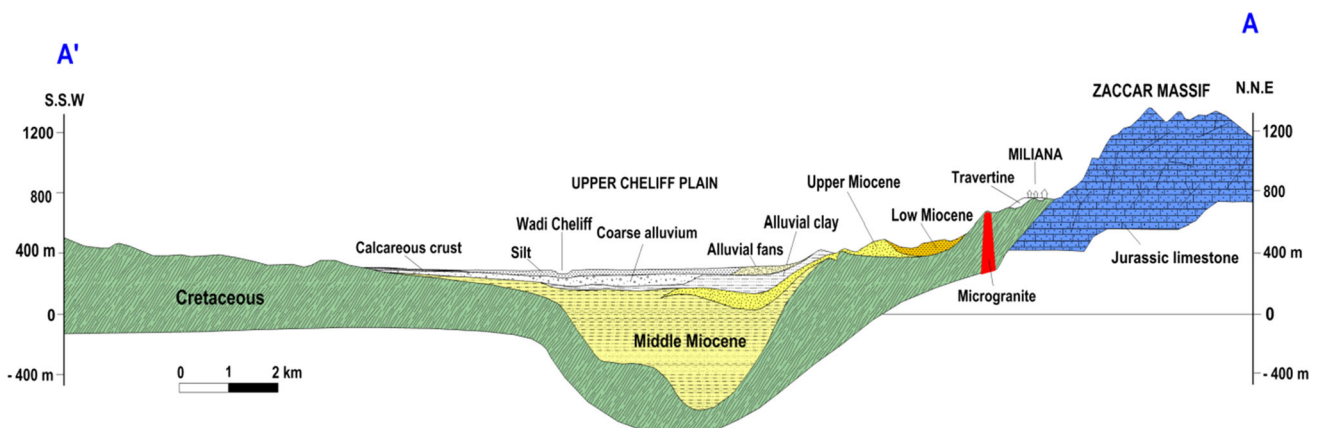

Fig. 2 Geological cross section A–A′ of the Upper Cheliff plain. Perrodon (1957), modified
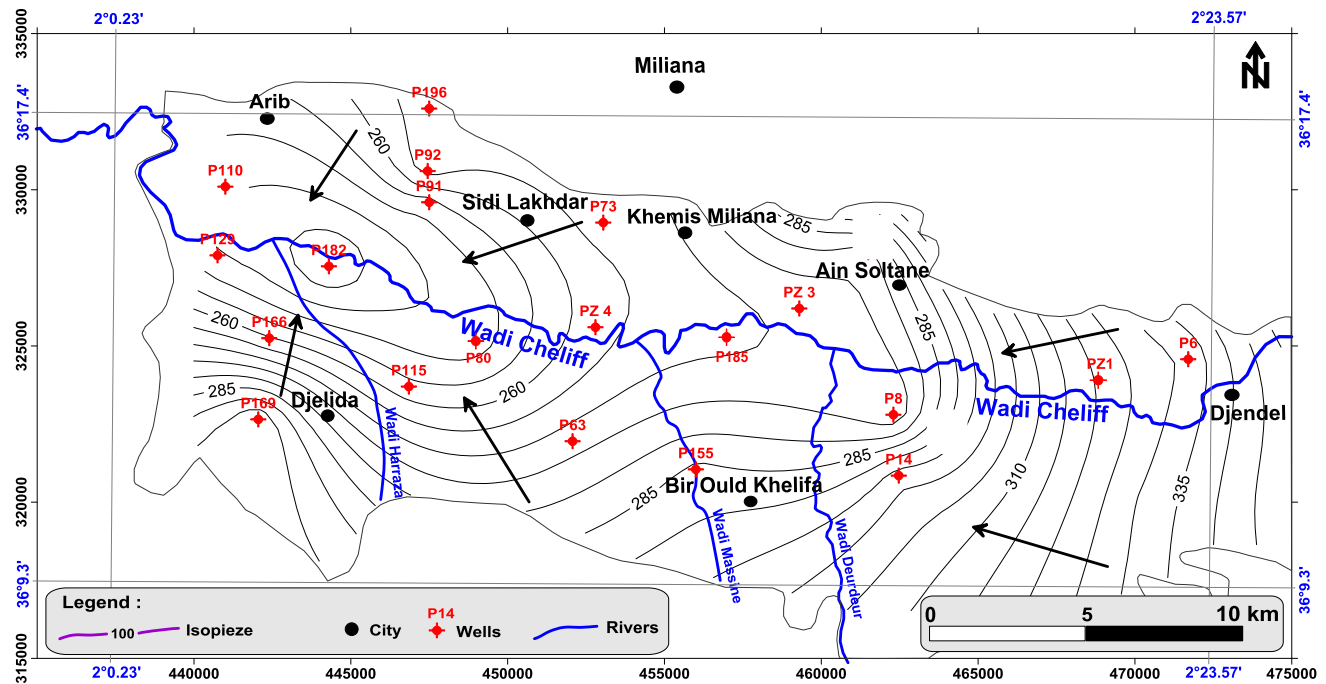
Fig. 3 Groundwater level contour map of the Upper Cheliff plain, dry period 2014

laboratory of Algerian waters (ADE-Ain Defla). The four major cations Mg^{2+}, Ca^{2+}, Na^+ and K^+ were analyzed by atomic absorption spectrometry, while for the major anions, Cl^- and HCO_3^- were analyzed by volumetric method, SO_4^{2-} and NO_3^- by spectrophotometer and col-orimetric method, respectively. The sample analyses were checked by calculating the ionic balance error between the total concentration of cations and anions. The ionic balance was applied, where the observed errors are between ± 5%, indicating that the analyses are acceptable and reliable. The exact locations of the sampling wells are shown in Fig. 2.

Iso-concentration contour maps were used to cartography the saptial distribution of contents in this aquifer. Piper plot was used to study the groundwater quality parameters in the study area; it is one of the most widely used techniques for visualizing the groundwater chemistry data (Peeters 2013). The principal component analysis (PCA) was also used on the chemical data for better understanding the groundwater hydrochemistry. The mechanism controlling the groundwater chemistry was studied by using Gibb's diagram and ionic rations.

Results and discussion

Physical parameters

The results of groundwater samples analysis for the dry season 2014 are presented in Table 1. The pH ranges from 7.1 to 8.3; it suggests that all of samples are conformed to standards (WHO 2008) and that the groundwater in this area is slightly alkaline (pH > 7.0). This is probably due to the influence of infiltration coming from the alkaline surface.

The electrical conductivity (EC) values range from 1313 to 4980 µS/cm, with an average of 3041 µS/cm. So, more than 85% of water samples are exceeding the standard recommend by WHO (2008), i.e., 1500 µS/cm. They were not permissible and hazardous for drinking water. The TDS values follow a similar trend to EC, and they varies from 791 to 2926 mg/l, with an average of 1952 mg/l, indicating more than 85% of samples exceed the permissible limit of 1000 mg/l. According to the classification of groundwater based on TDS given by WHO (2008), only three samples have permissible quality for drinking, and the majority of samples have brackish quality with TDS > 1000 mg/l (Fig. 4). This is a result of the processes affecting the groundwater, as lithology of the aquifer, climate conditions and anthropological influences. The highest values of EC and TDS were located in the south part of the plain, near to wadi: Deurdeur, Harreza and Massine. It is due probably to the influence of organic pollution (discharge of untreated sewage and the use of septic tank). The total hardness concentration varies from 45 to 147 °F. It reveals that the majority of wells (90%) in the study area have very hard quality (TH > 54 °F), and it could be related to the high concentrations of calcium and magnesium derived from the dissolution of calcareous crust.

Table 1 Results of physical and chemical analyses of groundwater (dry season 2014)

Wells	pH	EC (µS/cm)	TDS (mg/l)	TH (°F)	Ca^{2+} (mg/l)	Mg^{2+} (mg/l)	Na^+ (mg/l)	K^+ (mg/l)	Cl^- (mg/l)	SO_4^{2-} (mg/l)	HCO_3^- (mg/l)	NO_3^- (mg/l)
P8	7.5	3330	1899	113	331	72	189	6	800	281	275	76.0
P155	8.1	4980	2926	147	430	95	165	6	898	413	366	45.0
P14	7.3	3450	2142	135	402	82	143	4	740	198	250	65.0
P63	7.3	4080	2501	143	407	99	204	3	785	392	329	20.0
P73	7.4	3620	2412	131	372	91	203	6	595	440	339	26.0
P80	7.5	4750	2915	139	385	103	290	9	1070	463	299	12.0
P91	7.8	2350	1521	100	283	69	107	20	288	460	293	12.0
P92	7.2	1928	1434	73	208	51	91	3	268	192	305	83.0
P110	7.1	1313	791	45	144	21	47	4	168	47	290	27.0
P169	7.7	3650	2256	122	356	80	237	3	890	130	195	41.0
P182	7.2	2720	2186	100	264	81	147	3	398	284	427	24.0
P185	7.3	3420	2185	115	298	96	212	19	588	275	442	2.0
P196	7.3	1369	834	57	155	44	46	3	82	148	415	23.0
P6	7.3	2580	1659	92	267	60	136	3	381	129	378	150.0
PZ1	8.3	2720	1691	77	187	73	250	16	298	445	686	37.0
PZ2	7.3	4060	2508	138	398	93	273	6	888	230	351	37.0
PZ4	7.2	3170	2416	125	354	88	108	3	463	451	332	23.0
P129	7.4	2000	1324	75	189	66	75	13	253	300	320	99.0
P166	7.4	1446	944	54	146	41	61	12	215	112	290	78.0
P115	7.8	3890	2500	94	231	86	315	5	438	648	275	66.0

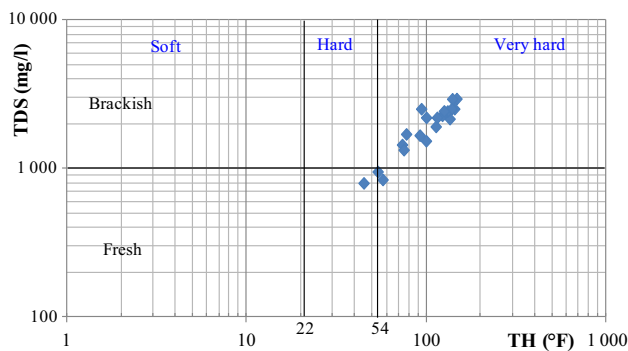**Fig. 4** Plot of TDS (mg/l) versus TH (°F)

Chemical parameters

The concentrations of individual anions in dry season vary from (Cl^- 82–1070 mg/l); SO_4^{2-} (47–648 mg/l); HCO_3^- (195–686 mg/l); NO_3^- (2–150 mg/l). The order of the relative abundance of major anions, expressed in percent of meq/L, was Cl^- (75%) > HCO_3^- (15%) > SO_4^{2-} (10%).

The high bicarbonate concentrations in this area can be due to the dissolution of carbonate minerals and the quaternary calcareous crust developed in the southern boundary of the Cheliff plain. It can also be due to the occurrence of oxidation of organic matter of the soil layers at emerging land (Odukoya 2015).

The contents of chlorides in the study area indicate more than 85% of samples exceed the standard limit fixed by WHO 250 mg/l. The very high concentrations of chlorides were observed in the south of the plain, particularly along Deurdeur and Massine wadis; this is probably due to the dissolution of NaCl salts observed in the south of the study area in Ouarsenis Mountain, and they are transported by these wadi toward the aquifer (recharge area). On the other hand, it comes probably from discharge of untreated sewage, while the enormous septic tanks in this sector exist in this part of the plain. Adding to that, the wastewater discharge from the different cities in this region is wadi Cheliff and its tributaries. However, the high values in the centre of the plain can be explained by the flow direction of groundwater as well as the residence time and the reactions that take place within the system (accumulation of salts). The high content of chloride in groundwater is due probably also to the infiltration of excess irrigation water, moderately mineralized (Fig. 5).

The highest values of sulfate concentrations of groundwater show more than 65% of wells exceed the standard fixed by OMS (200 mg/l). They may be due to the effect of the use of fertilizers in agriculture practices, the evaporation, wastewater discharge and to the dissolution of gypsum outcropping in the south part of the study area (in Ouarsenis Mountain) (Fig. 6).
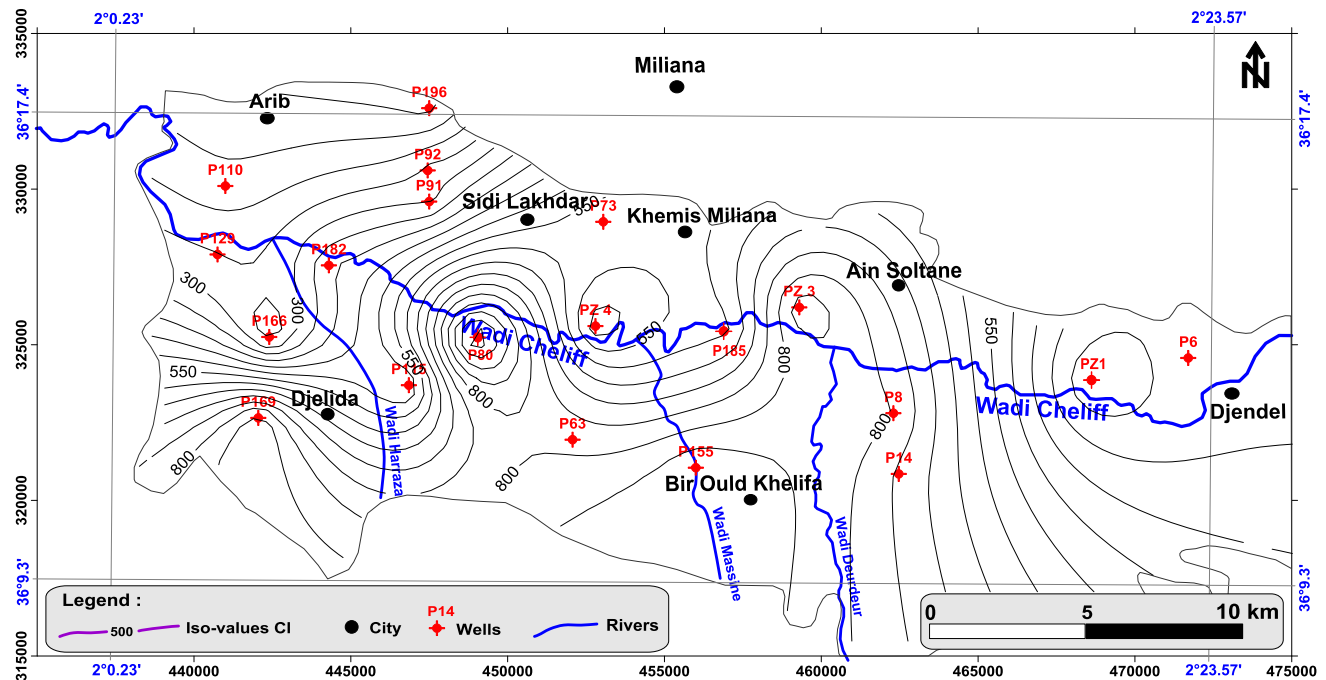
Fig. 5 Iso-concentration contour map of chloride ion (mg/l) in groundwater of the Upper Cheliff plain (dry period 2014)
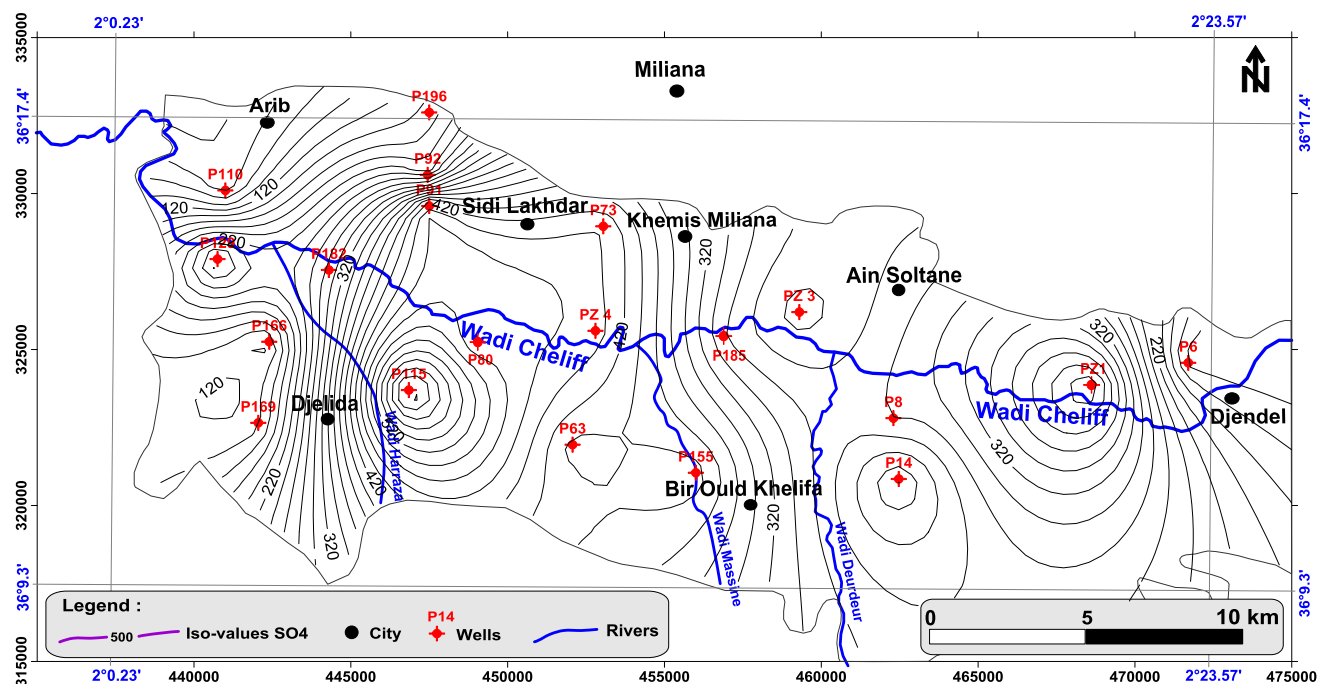

Fig. 6 Iso-concentration contour map of sulfate ion (mg/l) in groundwater of the Upper Cheliff plain (dry period 2014)

The nitrate concentrations in the study area (Fig. 7) show that the majority of the area have values between 50 and 160 mg/l, exceeding the limit of 50 mg/l established by the World Health Organization standards (WHO 2008). They can be attributed to the excess of using fertilizers in agricultural activities (The arboricultural and vegetable cultures occupy the most part of the Upper Cheliff plain). The highest nitrate concentrations are observed in the western part of the study area, especially in the irrigated zones located in the old quaternary formations represented by a conglomerate and pebble, calcareous crust and the alluvial fans, which are characterized by high
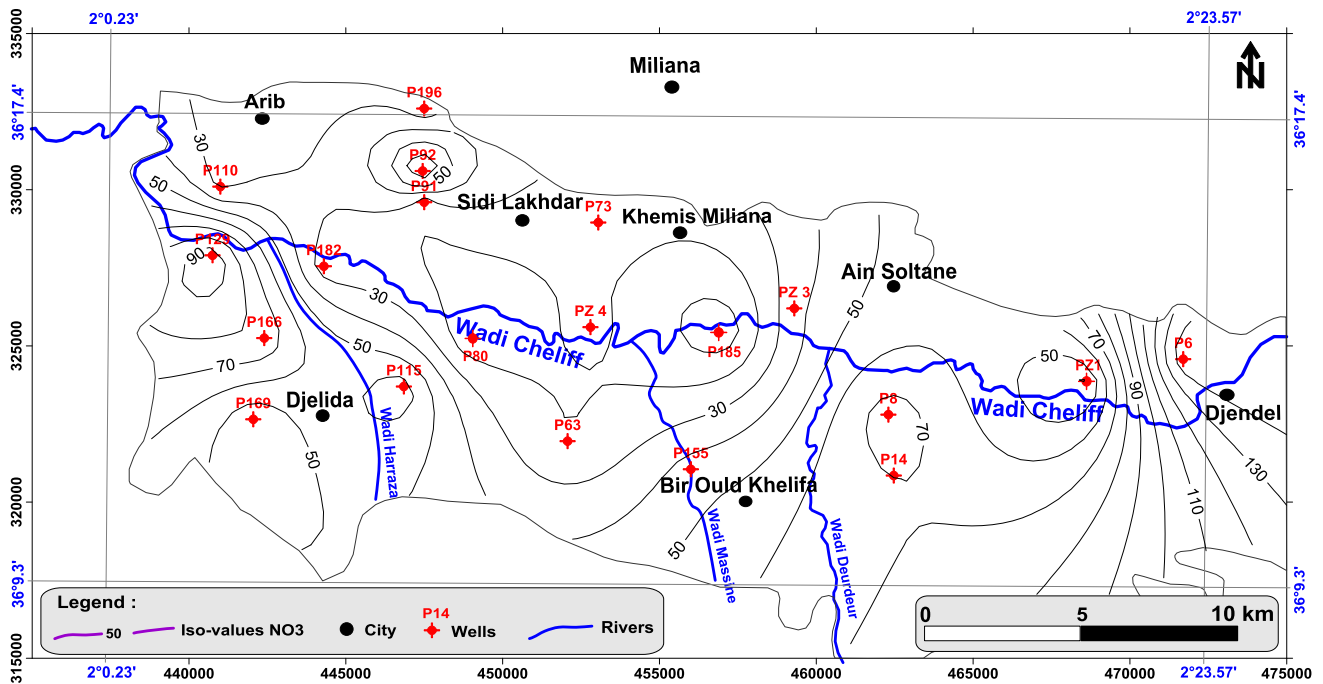
Fig. 7 Iso-concentration contour map of nitrate ion (mg/l) in groundwater of the Upper Cheliff plain (dry period 2014)

permeability. On the other side, the lower concentrations of nitrate observed in the center of the plain (< 50 mg/l) could be explained by the high thickness of an impermeable soil (clay) of recent alluvial formed by silt and clay (over 10 m).

However, wastes of animal origin, manure, soils containing nitrogen compounds, etc. can make another source of nitrate in the study area.

The concentration of major cations in groundwater samples during the dry period 2014 was varied from, Ca^{2+} (144–430 mg/l); Mg^{2+} (21–103 mg/l); Na^+ (64–315 mg/l) and K^+ (3–20 mg/l). The order of the relative abundance of major cations, expressed in percent of meq/l, was $Ca^{2+} > Na^+ > Mg^{2+} > K^+$.

The majority of the wells in this area have high concentrations of Ca^{2+} (more of 75%) compared to WHO guidelines (200 mg/l) (Fig. 8). They are due to the lithological deposits on the surface (dissolution of calcareous crust) and the dissolution of the consolidated detrital sedimentary rocks (dissolution of calcareous cement).

The very high levels of calcium in drinking water have some negative health effects. They promote vascular degeneration (arteriosclerosis) and osseus degenerative (osteoarthritis), and may adversely affect the absorption of other essential minerals in the human body, while the high levels of magnesium may give undesirable tastes for drinking water and may cause a change in bowel habits (diarrhea) (Arabi et al. 2013; Panhwar et al. 2014).

In the study area, more than 40% of samples exceed WHO guidelines (200 mg/l); it is probably due to the organic pollution (untreated wastewater discharge) accompanied to the leaching of fertilizers used in agricultural activities. The concentrations increase also if the residence time in groundwater increases or by pollution from sewage effluents. High contents of sodium in drinking water can be a problem for people whose have kidney, hypertension or heart disease problems.

In general, groundwater rarely has potassium levels more than 10 mg/l. Potassium results from the alteration of silicate formations (gneiss and schist), potassic clay and the percolation of chemical fertilizers toward the groundwater (intensive fertilization used in agricultural activities, NPK); it can also result from domestic and industrial discharge. In the study area, more than 20% of samples in this area exceed the limit of 12 mg/l.

The correlation matrix is used to assess the relationships between the groundwater chemical parameters and gives insights on pollution for effective water quality management (Table 2). Strong positive correlations were observed between TDS and EC, Ca^{2+}, Mg^{2+}, Na^+ and Cl^-. Similar strong positive correlations were observed between EC and Ca^{2+}, Mg^{2+}, Na^+ and Cl^-. There is also a strong positive correlation between Ca^{2+}, Mg^{2+} and Cl^-. They are indicators of the significance of these parameters in groundwater chemistry of the study area (Mondal et al. 2011). The moderate positive correlations were observed between Mg^{2+} and Na^+ and Cl^-, which indicates that these
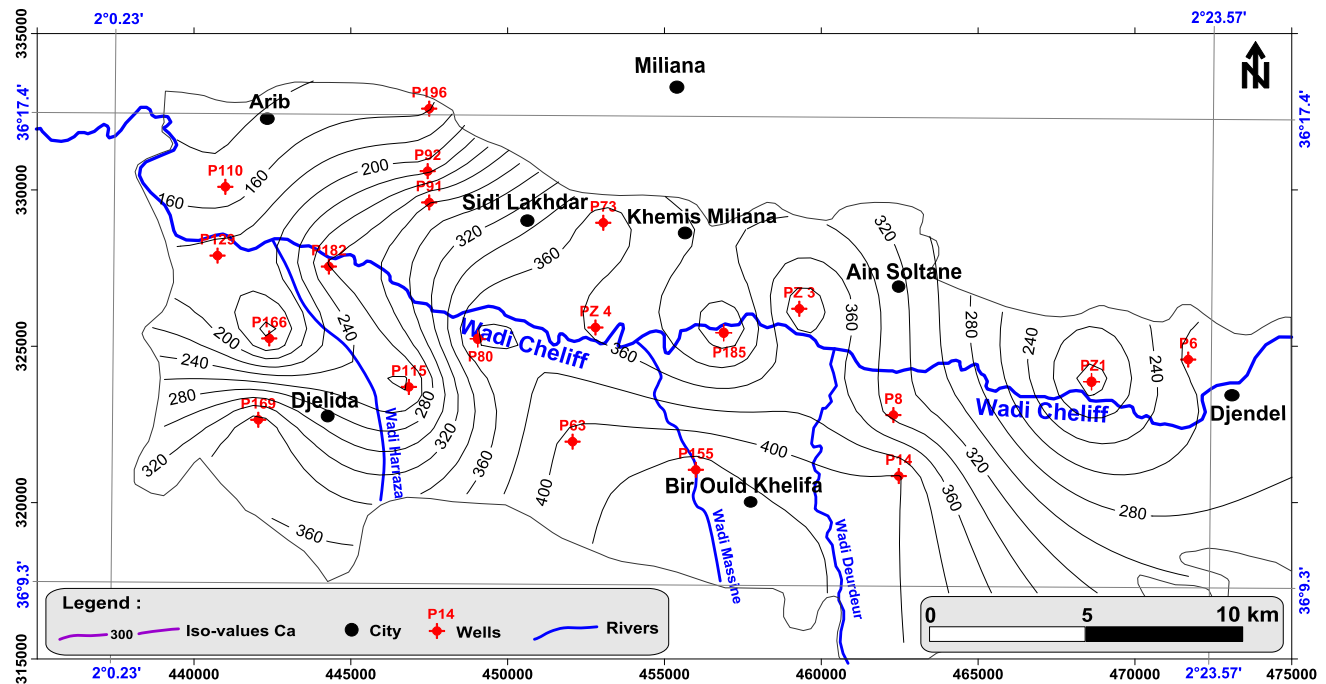
Fig. 8 Iso-concentration contour map of calcium ion (mg/l) in groundwater of the Upper Cheliff plain (dry period 2014)

Table 2 Correlation matrix of the hydrochemical parameters (dry period 2014)

	pH	TDS	EC	Ca^{2+}	Mg^{2+}	Na^+	K^+	HCO_3^-	Cl^-	SO_4^{2-}	NO_3^-
pH	1										
TDS	0.25	1									
EC	0.34	**0.97**	1								
Ca^{2+}	0.08	**0.87**	**0.88**	1							
Mg^{2+}	0.26	**0.94**	**0.91**	**0.83**	1						
Na^+	0.43	**0.77**	**0.80**	0.52	**0.75**	1					
K^+	0.41	− 0.15	− 0.11	− 0.21	0.06	0.05	1				
HCO_3^-	0.36	− 0.08	− 0.10	− 0.26	0.05	0.11	0.36	1			
Cl^-	0.16	**0.87**	**0.91**	**0.90**	**0.78**	**0.69**	− 0.17	− 0.28	1		
SO_4^{2-}	0.52	0.56	0.56	0.33	0.65	0.56	0.24	0.17	0.24	1	
NO_3^-	− 0.06	− 0.28	− 0.25	− 0.25	− 0.35	− 0.21	− 0.22	− 0.16	− 0.21	− 0.31	1

Bold values are significant correlation coefficients between parameters

parameters play also a role in defining the groundwater chemistry of this aquifer. The correlations between SO_4^{2-} and TDS, EC, Mg and Na ($r > 0.56$) have been identified which indicate that these ions control the groundwater chemistry in some wells in the study area.

The poor correlation of HCO_3^- with the other ions can be explained by the origin different of this ion with the other chemical parameters. HCO_3 can be derived from rainfall recharge, and NO_3^- can be derived from the fertilizers and manure used in agricultural practices. The pH values had low correlation with the other parameters in the groundwater and followed no consistent trend.

Hydrochemical facies

The groundwater chemistry in the Upper Cheliff plain was determined by plotting the samples on the Piper trilinear diagram (Piper 1953). Groundwater is represented as a solution of cationic constituents (Ca^{2+}, Mg^{2+} and alkali metals), anionic constituents (SO_4^{2-}, Cl^-) and constituents contributing to alkalinity (carbonate (CO_3^{2-}) and HCO_3^-). The groundwater types were determined by combining cation and anion fields.

As shown in the diamond part, the majority of groundwater samples fall in the zone III and IV, which suggests
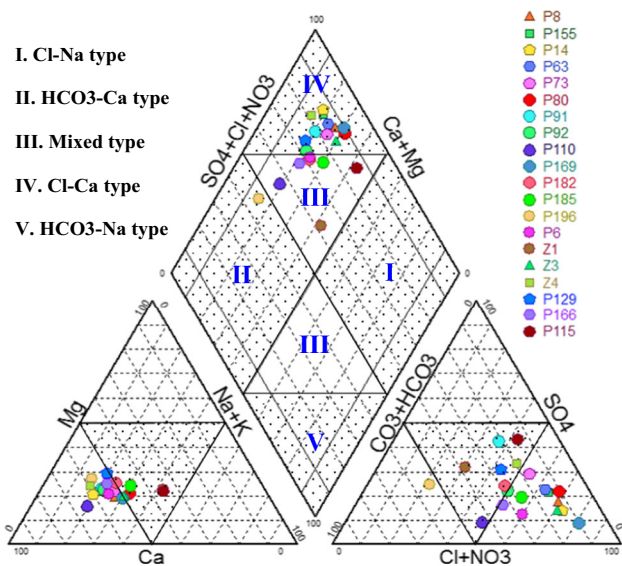
Fig. 9 Piper diagram showing hydrochemical facies of groundwater samples in the Upper Cheliff plain (dry period 2014)

Table 3 Varimax-rotated principal component matrices and the variables of the groundwater samples

Variables	Combined dataset		
	Component 1	Component 2	Component 3
pH	0.259	**0.774**	0.271
EC	**0.982**	0.063	− 0.033
Ca^{2+}	**0.912**	− 0.260	− 0.154
Mg^{2+}	**0.923**	0.147	− 0.216
Na^+	**0.817**	0.298	0.050
K^+	− 0.137	**0.744**	− 0.255
Cl^-	**0.926**	− 0.223	− 0.043
SO_4^{2-}	**0.560**	0.557	− 0.111
HCO_3^-	− 0.159	**0.724**	− 0.129
NO_3^-	− 0.218	− 0.166	**0.913**
Initial Eigen values of variances in %	46.179	21.901	10.762
Cumulative % of variance	46.179	68.080	**78.842**

that alkaline earth metals (Ca^{2+} + Mg^{2+}) exceeds alkalis (Na^+ + K^+) and strong acids anions (Cl^- + SO_4^{2-}) exceed weak acids anions (HCO_3^- + CO_3^{2-}). With respect to cations and anions, the majority of groundwater samples are indicating the dominance of Ca^{2+} and Cl^-, respectively. So, the dominant hydrochemical facies in this aquifer are Ca–Cl water type (60% of samples). However, the other samples have mixed facies (35% of samples) and Ca–HCO_3 water type (5% of samples) (Fig. 9).

The calcium chloride facies (Ca–Cl water type) are mainly linked to the geological origin (alluvial formations) and secondarily to the evaporation in the aquifer (semiarid climate area with depths of groundwater levels < 30 m) and can be due also to the anthropic influences (wastewater discharge and fertilizers infiltration). The bicarbonate–calcium facies (Ca–HCO_3) characterize one sample localized in the northwest of the study area (near to Arib city); it has an origin from carbonate formations. The mixed facies (Ca–Mg–SO_4–Cl/Ca–Na–SO_4–Cl) are linked to the combination of many parameters: the geological origin (ionic exchange between water-rock), evaporation, flow direction (accumulation of mineral salts) and anthropogenic effects.

Principal component analysis

Ten variables Ca^{2+}, Mg^{2+}, K^+, Na^+, Cl^-, SO_4^{2-}, HCO_3^-, NO_3^-, pH and EC were analyzed to obtain the principal components for the entire 20 samples collected in this plain. Varimax orthogonal rotation with Kaiser–Meyer–Olkin normalization was used to extract the principal components in the software SPSS.
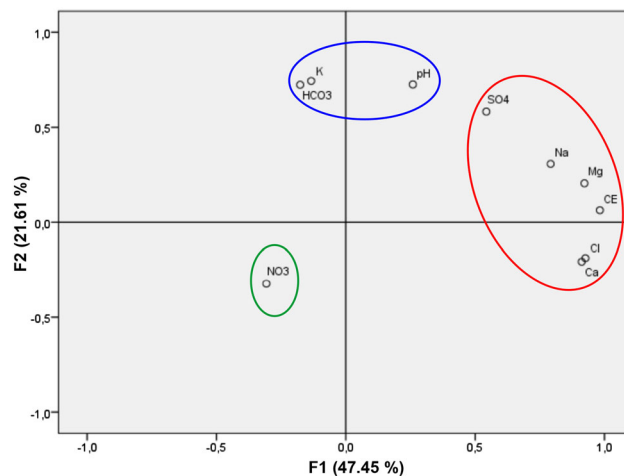

Fig. 10 Projection of the variables on the factor plan (1 x 2) of aquifer of Upper Cheliff

The scree plots show that three components (factors) have eigenvalues > 1, and these are the principal components extracted as shown in Table 3. The three principal components (factors) explain 78.842% of the total variance of data (Fig. 10). Factor loading is classified as strong, moderate and weak corresponding to absolute loading values of > 0.75, 0.75–0.50 and 0.50–0.30, respectively (Liu et al. 2003).

For the combined dataset, component 1 with the highest variance of 46.179% were reflecting the character of highly mineralized groundwater. The high positive loadings > 0.56 indicate that the parameters controlling the

groundwater chemistry are mainly Cl^-, Mg^{2+}, Ca^{2+}, SO_4^{2-} and Na^+. They have strong loadings, that are inferred to be related to the geoclimatic condition, complex natural processes and also the anthropogenic pollution. The component 2 explains 21.901% of total variance, with a strong positive loadings between pH, K^+ and HCO_3^-. The pH could be related to the changes in mineral compositions in groundwater as well as the mixing of rainwater with the groundwater through deep percolation. K^+ and HCO_3^- concentrations in the groundwater may be due to the dissolution of the minerals in the saturated and unsaturated zones. Factor 3 explains 10.762% of total variance, with a high positive loading of $NO_3^- > 0.913$, it can be inferred to the pollution may be linked to agricultural activities.

Mechanism controlling the groundwater chemistry

Evaporation and silicate weathering

The quality of groundwater depends on many factors such as infiltrating rainwater, geological structure and mineralogical composition of aquifer, dissolution and precipitation of mineral, seawater intrusion and anthropogenic influences (Singh et al. 2008; Tiwari and Singh 2014). Gibbs plot (1970) can be used to identify the three main hydrogeochemical processes controlling groundwater chemistry in an aquifer, such as evaporation/crystallization, and rock–water exchange.

Generally, a high concentration of Ca^{2+} and HCO_3^- denotes rock–water interaction, and high concentration of Na^+ and Cl^- reveals evaporation/crystallization processes, but we should take into account the depth of water table and the type of the aquifer (Tiwari et al. 2016).

Based on the Gibbs plots, the ratio of $(Na^+ + K^+)/(Na^+ + Ca^{2+} + K^+)$ and $Cl^-/(Cl^- + HCO_3^-)$ versus TDS indicates that the groundwater chemistry in the aquifer of Upper Cheliff is controlled by rock–water exchange and by evaporation during the dry period (Fig. 11). As the groundwater is obtained at shallow depth in many wells in the study area (depth < 10 m for wells located in the periphery of the plain and between 10 and 30 m for wells located in the center of the plain), direct evaporation is possible.

The Na^+/Cl^- versus EC plot is often used to identify and to distinguish the source of the salinity in groundwater, because these two chemical elements are often linked to the dissolution of halite (NaCl) (Sami 1992). In the study area, the Na^+/Cl^- ratios decrease when the EC increases (Fig. 12). They range from 0.28 to 1.29 (meq/l). The Na^+/Cl^- ratio lower than 1 indicates the reduction in sodium contents probably due to the ionic exchange of Na^+ for Ca^{2+} and Mg^{2+} in clays (Krishnaraj et al. 2011). The higher Na^+/Cl^- ratio (> 1.0) in some samples indicates a nonhalite source and suggests silicate weathering as a
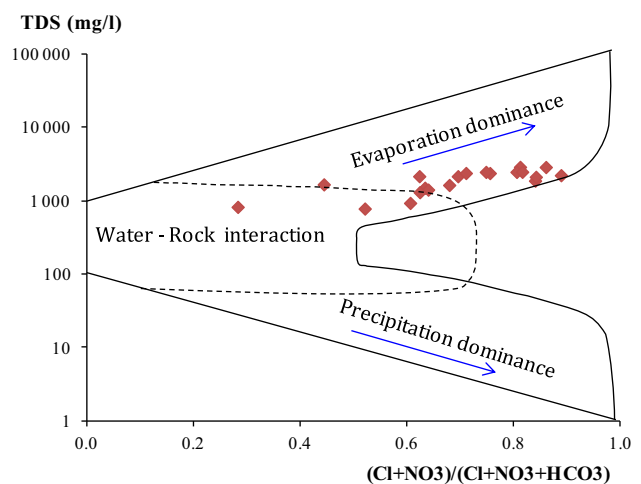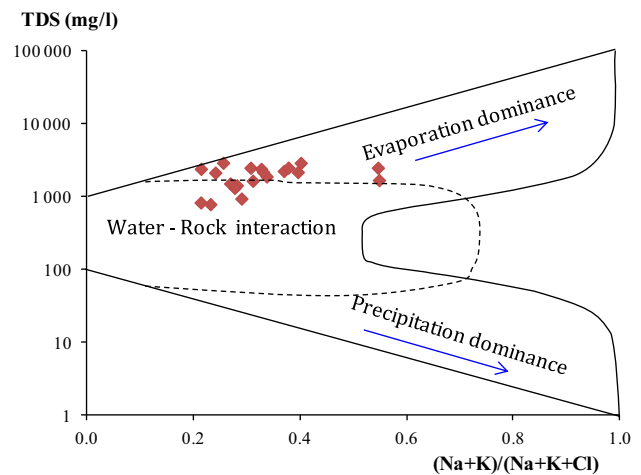

Fig. 11 Gibb's diagram illustrating mechanisms governing the chemistry of groundwater in Upper Cheliff plain (dry period 2014)

possible source of Na^+. If the evaporation process is dominant, assuming that no mineral species are precipitated, the Na^+/Cl^- ratio would be unaffected (Jankowski and Acworth 1997). Other sources of Na^+ and Cl^- in the groundwater of the study area may be domestic wastewater, which is usually enriched the Na^+ relatively to Cl^-.

Na^+ versus Cl^- has often used to identify the mechanism controlling salinity of groundwater. If Na^+ is released from halite dissolution, then the Na^+/Cl^- molar ratio will be approximately equal to 1, whereas ratio greater than 1 indicates silicate weathering (Hounslow 1995). In the study area, the Na^+-versus-Cl^- ratio plot (Fig. 13) indicates that the majority of samples fall above the freshwater evaporation line and less than equal line may be derived from a different anthropogenic origin. Two samples fall above the ratio greater than 1 and indicate the release of sodium due to silicate weathering, because there is no halite source in the plain, but bay be due to the sodium-based use of some fertilizers.
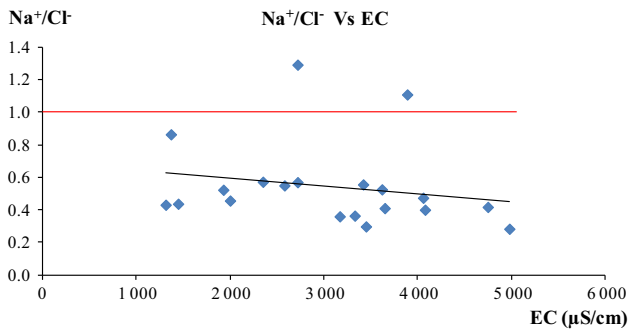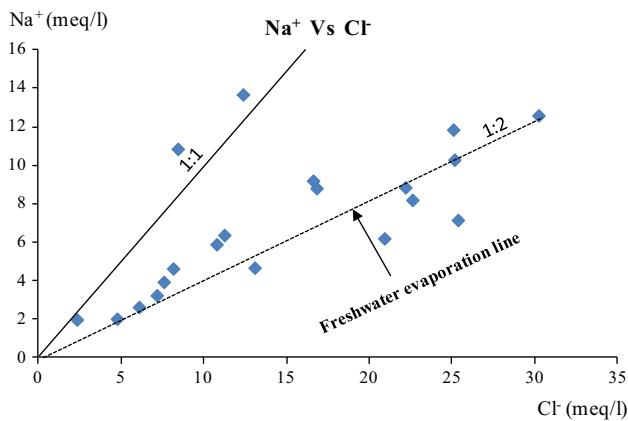
Fig. 12 Na$^+$/Cl$^-$ versus EC

Fig. 13 Na$^+$ versus Cl$^-$

Fig. 14 Plots of (Na$^+$ + K$^+$) and (Ca^{2+} + Mg^{2+}) versus total cation

The relationship between (Na$^+$ + K$^+$) and (Ca^{2+} + Mg^{2+}) with total cation was also used to verify the silicate weathering process. The ratio between Ca^{2+} + Mg^{2+} with total cation indicates that few samples fall near the Ca^{2+} + Mg^{2+} = 0.75 total cation line (Fig. 14). This indicates that the calcium and magnesium were much higher as compared with potassium and sodium suggesting that the major fraction of calcium and magnesium was derived from the weathering of carbonate rocks.

Ionic exchange process

To investigate further the process that affects calcium concentrations, the (Ca^{2+} + Mg^{2+}) versus HCO$_3^-$ for groundwater samples was used (Fig. 15). The most common weathering reaction in the case of carbonates is a simple dissolution, giving a 1:2 ratio of Ca/HCO$_3$. Low molar ratios (< 0.5) of Ca/HCO$_3$ indicate the exchange of calcium and magnesium in water by sodium in clay and/or cation exchange or HCO$_3$ enrichment possibly from silicate weathering. On the contrary, high ratios (> 0.5) suggest other sources for Ca and Mg, such as reverse ion exchange, which is observed in hard rock formations with an increase in salinity (Tziritis et al. 2016). In the study area, the
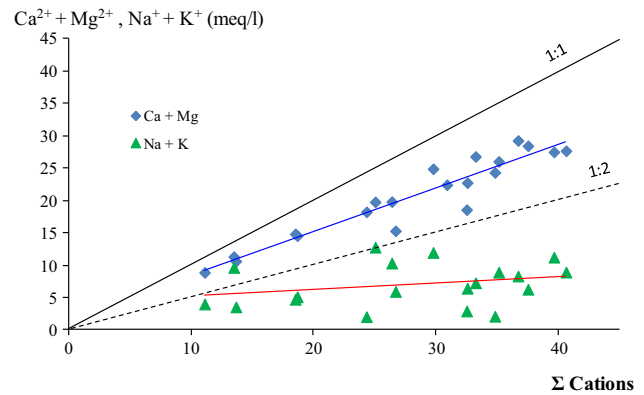
majority of samples fall above the 1:1 line, suggesting the excess of Ca^{2+} + Mg^{2+} shows that the carbonate weathering is dominant, which contributes Ca^{2+} and Mg^{2+} to groundwater (Kumar et al. 2011; Li et al. 2016). The molar ratio Ca^{2+} + Mg^{2+} ranges between 4.46 and 14.65, and it can be explained by the dissolution of the calcareous crust of quaternary (reverse ion exchange).

The plot of samples on the diagram Ca^{2+}/(HCO^{3-} + SO$_4^{2-}$) versus Na$^+$/Cl$^-$ (Fig. 16) shows that two samples undergo a basic exchange with an excess of Na$^+$, one sample indicates a natural state, and 65% of samples have an excess of Ca^{2+} relative to (HCO^{3-} + SO$_4^{2-}$) owed certainly by carbonate weathering that deliver more ions of Ca^{2+}.

The (HCO$_3^-$)/(Cl$^-$ + SO$_4^{2-}$) versus EC (Fig. 17) shows a decrease in this ratio when the electrical conductivity increase, which following a power equation tendency. Two different poles of samples can be observed in this area: The first one describes the natural state of samples. It is characterized by the dominance of HCO$_3^-$ with EC lower than 1500 μS/cm. The three (03) samples of this pole are located in the extreme downstream of the plain.

The second pole characterizes the anthropogenic pole with the dominance of Cl$^-$ and SO$_4^{2-}$ ions. The samples of this pole have EC > 1500 μS/cm, where the mineralization is coming from the different anthropogenic sources (agricultural practices, discharge of untreated sewage, etc.).

For better understanding the hydrogeochemical processes of groundwater in the Upper Cheliff plain, Chadha's diagram was used. It is based on the contents of major cations and anions. The data were converted to percentage reaction values (meq/l) and expressed as the difference between alkaline earth (Ca + Mg) and alkali metals (Na + K) for cations, and the difference between weak acidic anions (HCO$_3$ + CO$_3$) and strong acidic anions (Cl + SO$_4$) (Chadha 1999). The Chadha's plot (Fig. 18) indicates that only one sample falls on field 1 explained by the dominance of alkaline earth and weak acidic anions
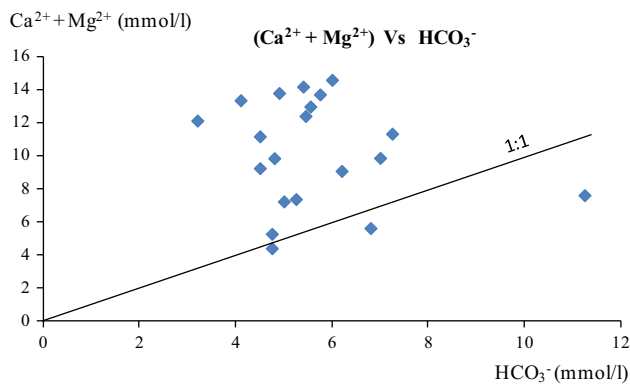
Fig. 15 Bivariate plot of $(Ca^{2+} + Mg^{2+})$ versus (HCO_3^-)

that exceed alkali metals and strong acidic anions as a result of Ca–Mg–HCO_3 water type, whereas the majority of groundwater samples fall in field 2, which show that alkaline earths exceed alkali metals and strong acidic anions exceed weak acidic anions; it is the consequence of reverse ion exchange process.

Mineral dissolution and precipitation

The ratio between $(Ca^{2+} + Mg^{2+})$ and $(SO_4^{2-} + HCO_3^-)$ specifies three hydrogeochemical processes such as samples close to 1:1 equal line that is explained by the dissolution of calcite and dolomite (Fisher and Mulican 1997). The samples above the equal line indicate an overload of $Ca^{2+} + Mg^{2+}$ which might be due to the reverse ion exchange process, and the samples below the equal line indicate an excess of $SO_4^{2-} + HCO_3^-$ due to ion exchange processes (Fig. 19a).

The bivariate plot of $[(Ca^{2+} + Mg^{2+})–(HCO_3^- +SO4^{2-})]$ versus $(Na^+–Cl^-)$ was used to establish the relationship between the ion exchange and reverse ion exchange processes
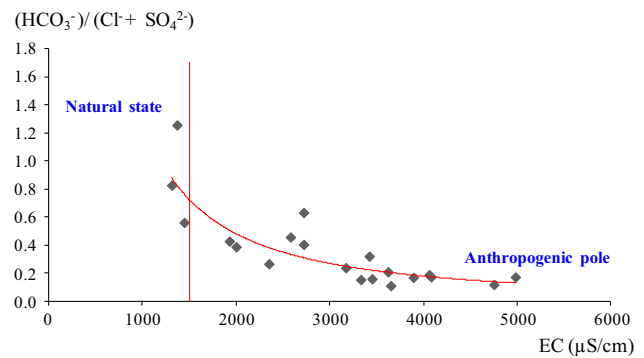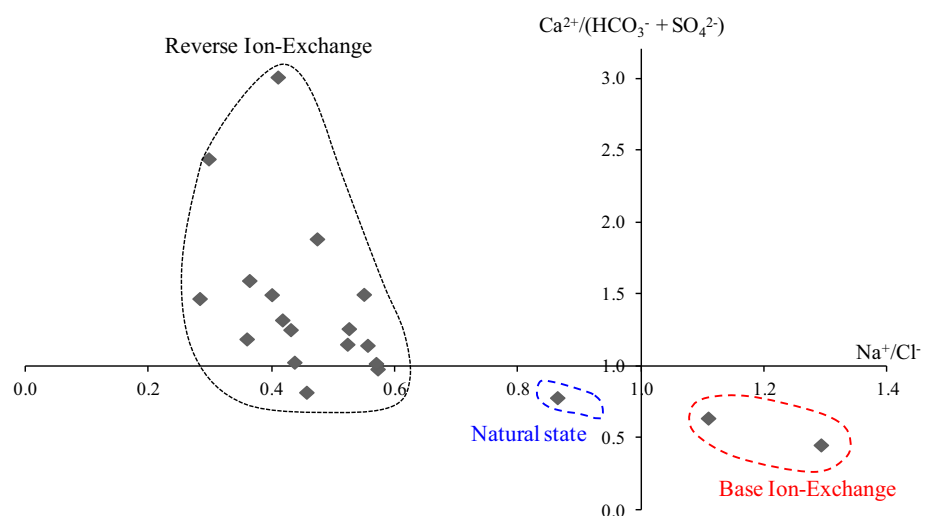

Fig. 17 Plots of $(HCO_3^-)/(Cl^- + SO_4^{2-})$ versus EC

(Rajmohan and Elango 2004). In the present study, the $[(Ca^{2+} + Mg^{2+})–(HCO_3^- +SO4^{2-})]$ versus $[(Na^+ + K^+)–Cl^-]$ plot indicates that the chemistry of the groundwater is controlled by reverse ion exchange process with a slope value of -0.5 (Fig. 19b).

Saturation index (SI) was used to predict the mineralogical reaction from groundwater data without collecting solid samples and mineralogical analysis. SI can help to identify the geochemical reactions that controlling water chemistry (Kumar 2014; Kanagaraj and Elango 2016). It is obtained from equation:

$$SI = \log(IAP/Kt) \tag{1}$$

where IAP is the ionic activity product of the solution and Kt is the equilibrium solubility product for the chemical involved at the sample temperature. The simulation is realized by the thermodynamic software PHREEQC. If the SI equal to zero, it reflects the solubility equilibrium with respect to the mineral phase of the water. SI less than zero indicates that groundwater is undersaturated with respect to this mineral and SI greater than 0 indicates that the groundwater is supersaturated with respect to the particular

Fig. 16 Plots of $Ca^{2+}/(HCO_3^- + SO_4^{2-})$ versus Na^+/Cl^-

Fig. 18 Chadha's diagram to assess the main hydrogeochemical processes in groundwater
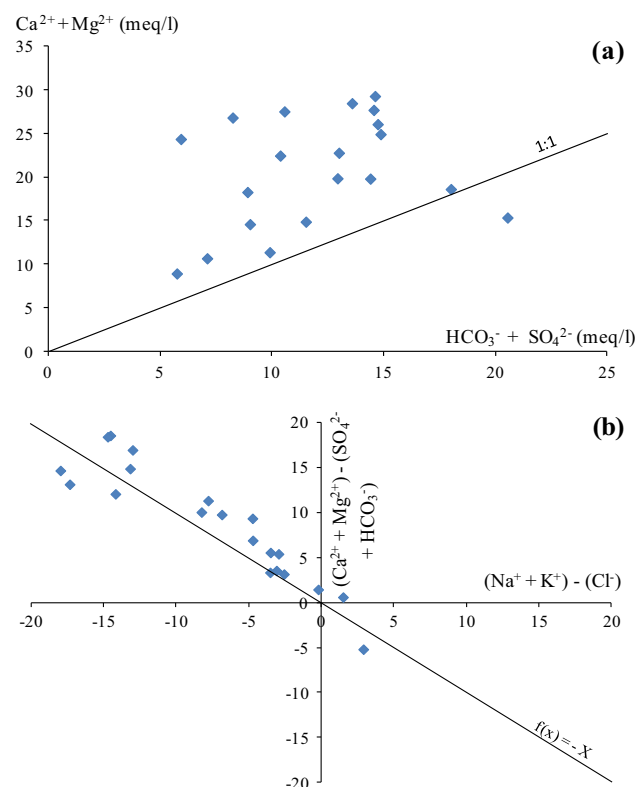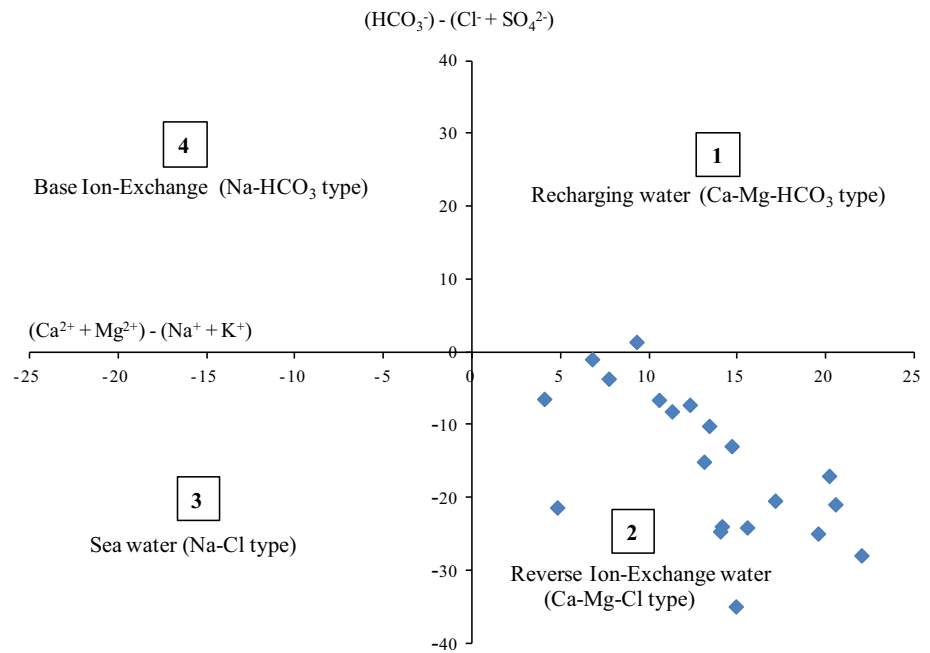

Fig. 19 Bivariate plot of **a** $(Ca^{2+} + Mg^{2+})$ versus $(SO_4^{2-} + HCO_3^-)$ and **b** $[(Ca^{2+} + Mg^{2+})–(HCO_3^- + SO_4^{2-})]$ versus $[(Na^+ + K^+)–Cl^-]$

mineral and is therefore unable to dissolve several minerals. Equilibrium is taken to be between SI $= -0.1$ and 0.1 (Bouderbala 2015). The saturation indices are shown in Fig. 20. The SI of aragonite, calcite and dolomite was positive (oversaturated), and they are ranged from 0.04 to 1.5, 0.18 to 1.64, and -0.12 to 3.23, respectively. Anhydrite, gypsum and halite were negative (undersaturated), and they are ranged from -1.96 to -0.89, -1.74 to -0.67 and -7.03 to -5.18, respectively.

In general, when the piezometric level increases, the saturation index of aragonite, calcite and dolomite increases also and becomes oversaturated in these minerals, suggesting that these carbonate mineral phases may have influenced the chemical composition of the study area.

The SI was compared with the Ca^{2+}/Mg^{2+} ratio. The Ca^{2+}/Mg^{2+} ratios will be 1 in the case of dolomite dissolution; the values from 1 to 2 specify the dissolution of calcite (Rajmohan and Elango 2006), and the values more than 2 are explained by the dissolution of silicate minerals (Kanagaraj and Elango 2016). The Ca^{2+}/Mg^{2+} ratios indicate in the study area 75% of the samples were falling above 2 indicating the effect of silicate weathering, which is explained by the high contents of calcium in groundwater (Fig. 20).

The saturation indices of calcite–aragonite and anhydrite–gypsum quietly coincide with each other.

The SI indicates also undersaturation of halite due to the dissolution of the mineral. It is confirmed by the negative saturation indices of groundwater. These salts are then leached under the influence of rainfall and irrigation water to reach the groundwater.

Assessment of groundwater quality for irrigation

The suitability of groundwater for irrigation use is assessed by EC, Cl, sodium absorption ratio (SAR), sodium

Fig. 20 Relationship between SI of anhydrite, aragonite, calcite, dolomite, gypsum, halite, groundwater level and Ca^{2+}/Mg^{2+} molar ratios of different wells
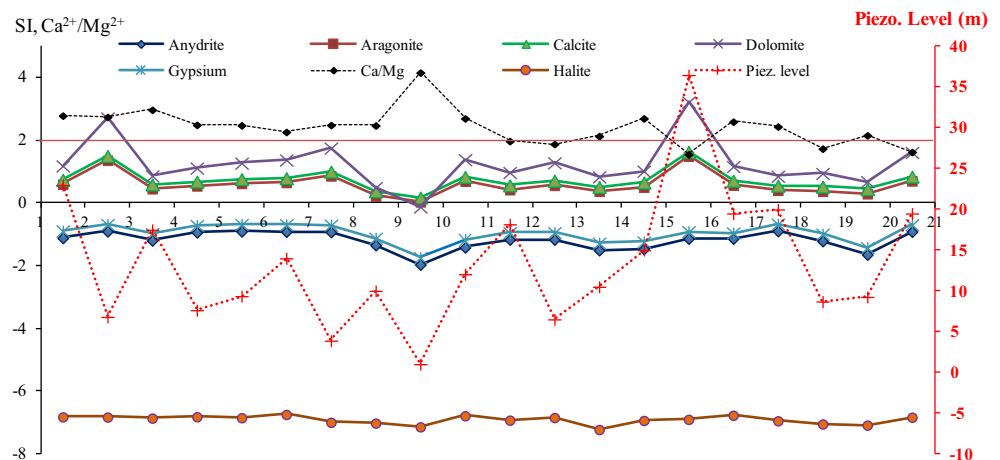
percentage (Na %), residual sodium carbonate (RSC), magnesium ratio (MR), Kelley's ratio (KR) and permeability index (PI) (Murkute 2014). They are calculated by the following equations:

$$SAR = Na^{+}/\sqrt{\left(Ca^{2+} + Mg^{2+}\right)/2} \qquad (2)$$

$$\%Na = \left[\left(Na^{+} + K^{+}\right)/\left(Ca^{2+} + Mg^{2+} + Na^{+} + K^{+}\right)\right] \times 100 \qquad (3)$$

$$RSC = \left(HCO_3^{-} + CO_3^{2-}\right) - \left(Ca^{2+} + Mg^{2+}\right) \qquad (4)$$

$$MR = \left[Mg^{2+}/\left(Ca^{2+} + Mg^{2+}\right)\right] \times 100 \qquad (5)$$

$$KR = Na^{+}/\left(Ca^{2+} + Mg^{2+}\right) \qquad (6)$$

$$PI = \left[\left(Na^{+} + \sqrt{HCO_3^{-}}\right)/\left(Ca^{2+} + Mg^{2+} + Na^{+}\right)\right] \times 100 \qquad (7)$$

where all ion concentrations are expressed in meq/l.

Electrical conductivity (EC) The results of the samples analysis of groundwater for the dry period 2014 indicate more than 55% of groundwater samples exceed 3000 μS/cm. The high value of EC has an impact on crop productivity and on the soil structure, because plants cannot transpire water. The amount of water transpired through a crop is directly related to yield; therefore, irrigation water with high EC reduces yield potential (Wilcox and Durum 1967).

Chlorides (Cl⁻) Chlorides move easily in the soil, but they are absorbed by crops and accumulate in the leaves, which create many symptoms. In the study area, more than 35% of samples exceed the limit of 12 meq/l, and they are unsuitable for irrigation.

Sodium adsorption ratio (SAR) This parameter quantifies the proportion of sodium (Na^{+}), calcium (Ca^{2+}) and

magnesium (Mg^{2+}) ions in a water sample. It should be noted that Na^{+} plays a negative role in the soil, because it reacts with the soil by decreasing its permeability and also decreasing the water flow in the soil. The values of SAR less than 13 indicate no danger from sodium, SAR from 13 to 22 indicates little danger from sodium and water has a medium quality, SAR from 22 to 32 indicates high hazards of sodium, while values of SAR more than 32 indicate very high hazards of sodium water are unsuitable for irrigation (Richard 1954). Sodium replaces adsorbed calcium and magnesium, which leads to damage to the soil structure owing to the dispersion of the clay particles, and the soil becomes compact with low permeability. The values of SAR range from 0.8 to 4.5 meq/l (Table 4), and their plots on Riverside's diagram show that groundwater samples fall in C3S1, C4S1 and C4S2 categories. Out of 20 groundwater samples analyzed, 25% fall under C3S1 class, indicating a moderate salinity hazard and low sodium water, which refers to permissible irrigation water for a crop of salt tolerant, with adequate drainage of soils or soils of good permeability; however, the salinity must be controlled. The C4S1 (55%) and C4S2 (20%) classes indicate poorly and mineralized irrigation waters, and they are only suitable for the irrigation of some crops that tolerant to salts and grown on good drained and leached soils or organic soils having a good permeability (Fig. 21).

Sodium percentage (% Na) It is based on the total concentration of dissolved salts and the percentage of sodium relative to other salts in water. The salts present in the groundwater can affect the growth of the plants directly, also deteriorate the soil structure and reduce its aeration and permeability (Joshi et al. 2009). The sodium percentage (% Na) in the study area ranges from 15.5 to 42.6 (Table 4), which indicate permissible groundwater quality for irrigation.

**Table 4** Irrigation quality results of groundwater samples from the Upper Cheliff plain (dry period 2014)

Wells	EC (µS/cm)	SAR	% Na	RSC	MR	KR	PI
P8	3330	2.45	27.12	−17.98	26.37	0.37	33.68
P155	4980	1.87	19.98	− 23.32	26.67	0.24	26.37
P14	3450	1.70	19.07	− 22.75	25.14	0.23	24.93
P63	4080	2.35	23.91	− 23.10	28.59	0.31	29.95
P73	3620	2.44	25.59	− 20.54	28.71	0.34	32.03
P80	4750	3.39	31.63	− 22.83	30.57	0.45	36.75
P91	2350	1.48	20.66	− 15.03	28.64	0.23	27.95
P92	1928	1.46	21.68	− 9.60	28.76	0.27	33.38
P110	1313	0.97	19.41	− 4.18	19.36	0.23	38.49
P169	3650	2.95	29.83	− 21.18	27.00	0.42	34.86
P182	2720	2.03	24.58	− 12.87	33.56	0.32	34.42
P185	3420	2.73	29.85	− 15.55	34.65	0.40	37.20
P196	1369	0.84	15.49	− 4.57	31.85	0.18	34.46
P6	2580	1.96	24.67	− 12.09	27.00	0.32	34.72
PZ1	2720	3.92	42.36	− 4.11	39.12	0.71	54.23
PZ2	4060	3.20	30.37	− 21.80	27.78	0.43	36.19
PZ4	3170	1.33	16.06	− 19.49	29.04	0.19	23.72
P129	2000	1.20	19.45	− 9.63	36.50	0.22	30.60
P166	1446	1.15	21.70	− 5.92	31.61	0.25	36.26
P115	3890	4.49	42.60	− 14.13	38.00	0.74	48.93

Residual sodium carbonate (RSC) It is a quick test to determine whether irrigation water can release free calcium and magnesium in the soil. The high bicarbonate contents in the water are due to the biological activities of plant roots and from the oxidation of organic matter included in the soils and in the rock, and from various chemical reactions (Raju 2007). In the study area, all the groundwater samples have RSC values lower than zero (Table 4), which can be used for irrigation without problems.

Permeability index (PI) The impact of irrigation water on the soil permeability can be evaluated by using permeability index which depends on the sodium, calcium, magnesium and bicarbonate contents (Raju 2007; Amiri et al. 2015). In the study area, the PI values of groundwater samples are lower than 75 (Table 4). The groundwater quality doesn't create any permeability problem.

Magnesium ratio (MR) In ordinary cases, excess magnesium in groundwater can reduce the soil structure, which influences the yield of crops (Arveti et al. 2011; Nagaraju et al. 2014). The computed values of groundwater samples in this area are between 19.4 and 39.1 (Table 4), which indicate water quality suitable for irrigation (MR < 50).

Fig. 21 Riverside's diagram for irrigation water classification
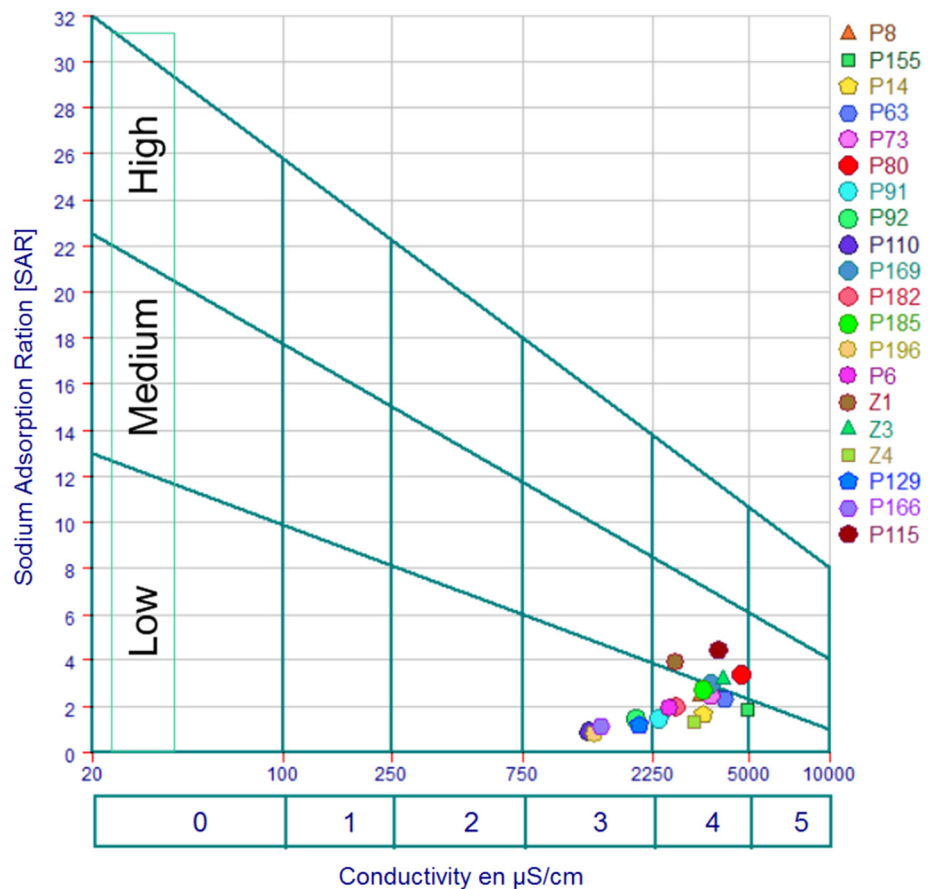
Kelly's ratio According to Kelly's ration, if the ratio is less than one the water is suitable for irrigation, whereas if the ratio is more than one the water is unsuitable for irrigation and it indicates that there is an excessive of sodium in water which could create a salinity problem in the soil. In the study area, groundwater is permissible for irrigation according to Kelly's ratio (Table 4).

Conclusion

The assessment of hydrogeochemical processes and the impact of anthropogenic pollution on groundwater quality was carried out based on the collection and analyses of groundwater samples for the dry period 2014, in the Upper Cheliff plain (northern Algeria).

The analyses of 20 samples distributed over the plain indicate slightly alkaline groundwater quality in this area in nature, with 85% of electrical conductivity higher than 1500 μS/cm due to high mineral concentration, which indicates that the ion exchange reactions and solubilization processes have occured within this aquifer. Cl^- and SO_4^{2-} dominate the groundwater in anionic concentration and Ca^{2+} and Mg^{2+} in the cationic abundances, which suggests that alkaline earth $(Ca + Mg)$ exceeds alkali metals $(Na + K)$ and strong acids $(Cl + SO_4)$ exceed weak acids $(HCO_3 + CO_3)$. Ca–Cl, and mixed facies (Ca–Mg–SO$_4$–Cl/Ca–Na–SO$_4$–Cl) and Ca–HCO$_3$ were the dominant hydrogeochemical groundwater facies. The use of the different ratios and principal component analysis (PCA) reveals that the combined effect of human activities related to the uses of organic fertilizer in agriculture, discharges of untreated wastewater and the use of domestic septic tanks by rural inhabitants are the major factors most responsible for the degradation of groundwater quality in this plain. Adding to that, geoclimatic conditions and the dissolution of the minerals in the saturated and unsaturated zones have also contributed to the mineralization of groundwater.

The saturation indices show supersaturated of calcite and dolomite for all groundwater samples due to the dissolution of carbonate mineral under rainfall and the infiltration of the excess of irrigation water, and undersaturated of halite is confirmed by the negative saturation indices of groundwater which due to the dissolution of this mineral.

The assessment of groundwater quality in this plain indicates poor quality with high amounts of Cl, SO$_4$, Ca and NO$_3$, EC, TDS and TH for the majority of groundwater samples, which makes more than 75% of groundwater samples unsuitable for domestic uses and more than 20% of samples unsuitable for irrigation due to the high salinity hazard which may a problem for soils textured.

References

Amiri V, Sohrabi N, Dadgar MA (2015) Evaluation of groundwater chemistry and its suitability for drinking and agricultural uses in the Lenjanat plain, central Iran. Environ Earth Sci 74:6163–6176

Arabi AS, Funtua II, Dewu BBM, Garba ML, Okoh S, Kwaya MY, Bolori MT (2013) Assessment of calcium and magnesium concentrations in groundwater as supplements for sleep related ailments. J Appl Environ Biol Sci 3(7):29–35

Arveti N, Sarma MRS, Aitkenhead-Peterson JA, Sunil K (2011) Fluoride incidence in groundwater: a case study from Talupula, Andhra Pradesh, India. Environ Monit Asses 172:427–443

Bouderbala A (2015) Groundwater salinization in semi-arid zones: an example from Nador plain (Tipaza, Algeria). Environ Earth Sci 73(9):5479–5496

Bouderbala A (2017) Assessment of water quality index for the groundwater in the upper Cheliff plain, Algeria. J Geol Soc India 90(3):347–356

Chadha DK (1999) A proposed new diagram for geochemical classification of natural waters and interpretation of chemical data. Hydrogeol J 7(5):431–439

Fisher RS, Mulican WFIII (1997) Hydrochemical evaluation of sodium-sulphate and sodium-chloride groundwater beneath the northern Chihuahuan desert, trans-Pecos, Texas USA. Hydrogeol J 10:455–474

Gibbs RJ (1970) Mechanisms controlling worlds water chemistry. Science 170:1088–1090

Hounslow AW (1995) Water quality data: analysis and interpretation. CRC Lewis Publishers, New York

Jankowski J, Acworth RI (1997) Impact of debris-flow deposits on hydrogeochemical processes and the developement of dryland salinity in the Yass River catchment, New South Wales, Australia. Hydrogeol J 5(4):71–88

Joshi DM, Kumar A, Agrawal N (2009) Assessment of the irrigation water quality of river Ganga in Haridwar District. Rasayan J Chem 2(2):285–292

Kanagaraj G, Elango L (2016) Hydrogeochemical processes and impact of tanning industries on groundwater quality in Ambur, Vellore district, Tamil Nadu, India. Environ Sci Pollut Res 23(23):24364–24383

Khatri N, Tyagi S (2015) Influences of natural and anthropogenic factors on surface and groundwater quality in rural and urban areas. Front Life Sci 8(1):23–39

Krishnaraj S, Murugesan V, Vijayaraghavan K, Sabarathinam C, Paluchamy A, Ramachandran M (2011) Use of hydrochemistry and stable isotopes as tools for groundwater evolution and contamination investigations. Geosciences 1(1):16–25

Kumar PS (2014) Evolution of groundwater chemistry in and around Vaniyambadi industrial area: differentiating the natural and anthropogenic sources of contamination. Chemie der Erde-Geochemistry 74(4):641–651

Kumar PS, Jegathambal P, James EJ (2011) Multivariate and geostatistical analysis of groundwater quality in Palar river basin. Int J Geol 4:108–119

Li P, Zhang Y, Yang N, Jing L, Yu P (2016) Major ion chemistry and quality assessment of groundwater in and around a mountainous tourist town of China. Expos Health 8(2):239–252

Liu CW, Lin KH, Kuo YM (2003) Application of factor analysis in the assessment of groundwater quality in a blackfoot disease area in Taiwan. Sci Total Environ 313(1):77–89

Mattauer M (1958) Etude géologique de l'Ouarsenis oriental, Algérie. Publication service carte Algérie Thèse université Franche Comté, Besançon (France)

Meghraoui M (1982) Etude néotectonique de la région nord-est d'El Asnam: relation avec le séisme du 10 octobre 1980. Thèse université de Paris VII (France)

Mohsen J (2011) Hydrogeochemistry of groundwater and its suitability for drinking and agricultural use in Nahavand, western Iran. Nat Resour Res 20:65–73

Mondal NC, Singh VP, Singh VS, Saxena VK (2010) Determining the interaction between groundwater and saline water through groundwater major ions chemistry. J Hydrol 388:100–111

Mondal NC, Singh VS, Saxena VK, Singh VP (2011) Assessment of seawater impact using major hydrochemical ions: a case study from Sadras, Tamilnadu, India. Environ Monit Assess 177(1–4):315–335

Murkute YA (2014) Hydrogeochemical characterization and quality assessment of groundwater around Umrer coal mine area Nagpur District, Maharashtra, India. Environ Earth Sci 72:4059–4073

Nagaraju A, Kumar KS, Thejaswi A (2014) Assessment of groundwater quality for irrigation: a case study from Bandalamottu lead mining area, Guntur District, Andhra Pradesh, South India. Appl Water Sci 4(4):385–396

Odukoya AM (2015) Geochemical and quality assessment of groundwater in some Nigerian basement complex. Int J Environ Sci Technol 12:3643–3656

Panhwar AH, Kazi TG, Afridi HI, Talpur FN, Arain S, Kazi N (2014) Distribution of potassium, calcium, magnesium, and sodium levels in biological samples of Pakistani hypertensive patients and control subjects. Clin Lab 60(3):463–474

Peeters L (2013) A background color scheme for piper plots to spatially visualize hydrochemical patterns. Groundwater 52(1):2–6

Perrodon A (1957) Etude géologique des bassins néogènes sublittoraux de l'Algérie Nord occidentale. Thèse université de Paris VII (France), Publications du service de la carte géologique de l'Algérie, 12

Piper AM (1953) A graphic procedure in the geochemical interpretation of water analysis. United States Geological Survey, Washington

Pulido-Madrigal L, Simuta-Champo R, González-Meraz J, Saucedo H (2012) Producción Agrícola Sustentable en Condiciones de Sobreexplotación de Agua Subterránea. Terra latinoamericana 30(4):303–313

Raj D, Shaji E (2016) Fluoride contamination in groundwater resources of Alleppey, southern India. Geosci Front 8:117–124

Rajmohan N, Elango L (2004) Identification and evolution of hydrogeochemical processes in the groundwater environment in an area of the Palar and Cheyyar River Basins, southern India. Environ Geol 46(1):47–61

Rajmohan N, Elango L (2006) Hydrogeochemistry and its relation to groundwater level fluctuation in the Palar and Cheyyar river basins, southern India. Hydrol Process 20(11):2415–2427

Raju NJ (2007) Hydrogeochemical parameters for assessment of groundwater quality in the upper Gunjanaeru River basin, Cuddapah District, Andhra Pradesh, south India. Environ Geol 52(6):1067–1074

Richard LA (1954) Diagnosis and improvement of saline and alkali soils. Agricultural Handbook, vol 60. USDA, Washington DC

Saleem M, Jeelani G, Shah RA (2015) Hydrogeochemistry of Dal Lake and the potential for present, future management by using facies, ionic ratios, and statistical analysis. Environ Earth Sci 74:3301–3313

Sami K (1992) Recharge mechanisms and geochemical processes in a semi-arid sedimentary basin, Eastern Cape, South Africa. J Hydrol 139:27–48

Singh AK, Mondal GC, Kumar S, Singh TB, Tewary BK, Sinha A (2008) Major ion chemistry, weathering processes and water quality assessment in upper catchment of Damodar River basin, India. Environ Geol 54:745–758

Subramani T, Rajmohan N, Elango L (2010) Groundwater geochemistry and identification of hydrogeochemical processes in a hard rock region, Southern India. Environ Monit Assess 162:123–137

Tiwari AK, Singh AK (2014) Hydrogeochemical investigation and groundwater quality assessment of Pratapgarh District, Uttar Pradesh. J Geol Soc India 83(3):329–343

Tiwari AK, De Maio M, Singh PK, Singh AK (2016) Hydrogeochemical characterization and groundwater quality assessment in a coal mining area, India. Arab J Geosci 9(3):1–17

Touhari F, Meddi M, Mehaiguene M, Razack M (2015) Hydrogeochemical assessment of the upper cheliff groundwater (North West Algeria). Environ Earth Sci 73(7):3043–3061

Tziritis E, Skordas K, Kelepertsis A (2016) The use of hydrogeochemical analyses and multivariate statistics for the characterization of groundwater resources in a complex aquifer system. A case study in Amyros River basin, Thessaly, central Greece. Environ Earth Sci 75(4):1–11

WHO World Health Organization (2008) Guidelines for drinking-water quality, 2nd edn. WHO, Geneva

Wilcox LV, Durum WH (1967) Quality of irrigation water. In: Hagan RM, Haise HR, Edminster TW (eds) Irrigation of agricultural lands, vol 11. American Society of Agronomy, Monograph, pp 104–122